We consider time evolution using 'time-dependent variational principle' (TDVP)

1. 1-site TDVP [Haegeman2016, App. B]

Schrödinger equation for MPS:

$$i\frac{d}{dt}|\tilde{\Psi}[M(t)]\rangle = \hat{H}\,|\Psi[M(t)]\rangle \qquad (1)$$

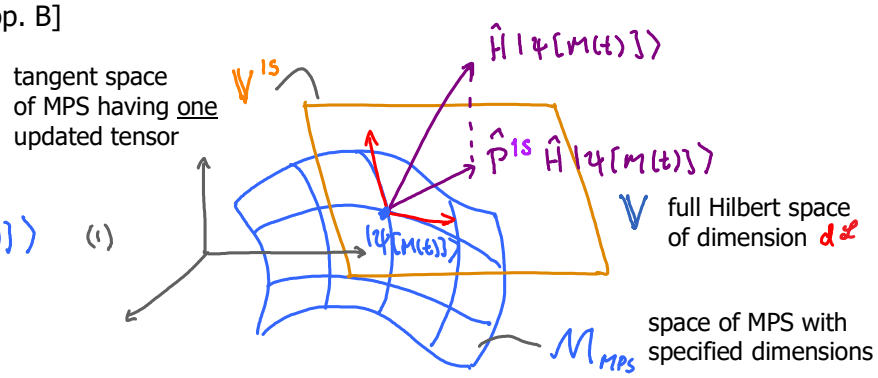

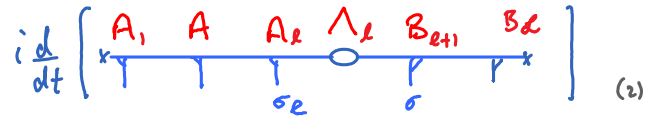

(2)

if we insist on using MPS with fixed bond dimensions, left side has following form:

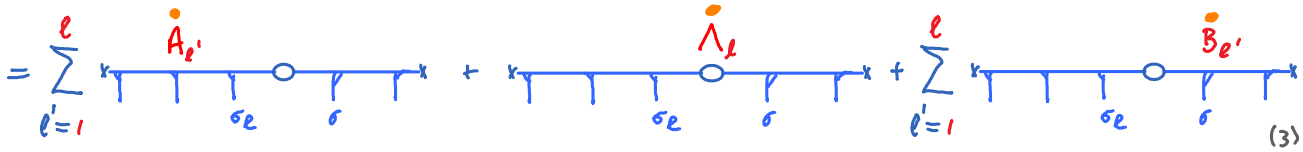

(3)

Each term differs from $|\tilde{\Psi}(t)\rangle$ by precisely one site tensor or on bond tensor, so left side is a state in the tangent space, $\mathbb{V}^{1s}$ of $|\Psi(t)\rangle$. But right side of (1) is not, since since $H|\Psi(t)\rangle$ can have larger bond dimensions than $|\Psi(t)\rangle$.

So, project right side of (1) to $\mathbb{V}^{1s}$:

$$i\frac{d}{dt}|\tilde{\Psi}[M(t)]\rangle \simeq \hat{P}^{1s}\,\hat{H}\,|\Psi[M(t)]\rangle \qquad (4)$$

(≃: tangent space approximation)

Left and right sides of (4) are structurally consistent. To see this, consider bond ℓ

Left side of (4) contains:

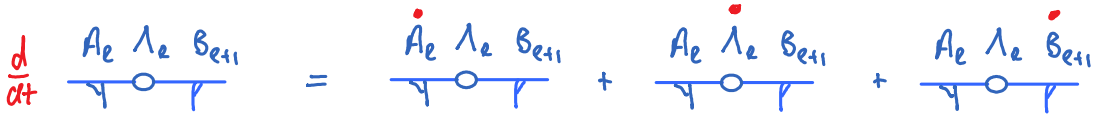

(5)

Decompose: $\dot{A}_\ell = A_\ell \Lambda'_\ell + \bar{A}_\ell \bar{\Lambda}'_\ell$, $B_{\ell+1} = \Lambda''_\ell B_{\ell+1} + \bar{\Lambda}'' \bar{B}_{\ell+1}$ (6)

Then we find:

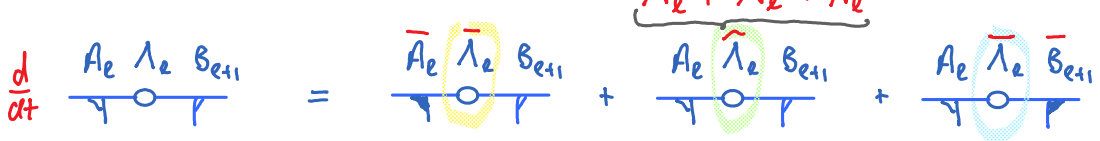

(7)

Right side of (4) requires tangent space projector. Consider its form (TS-I.5.25):

(8)

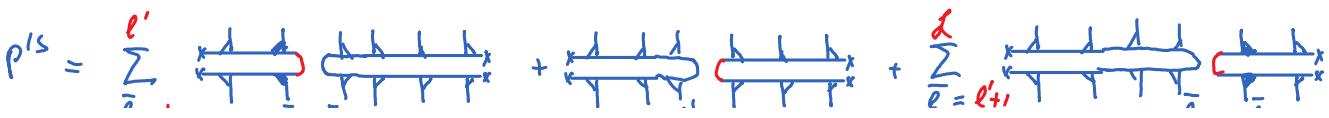

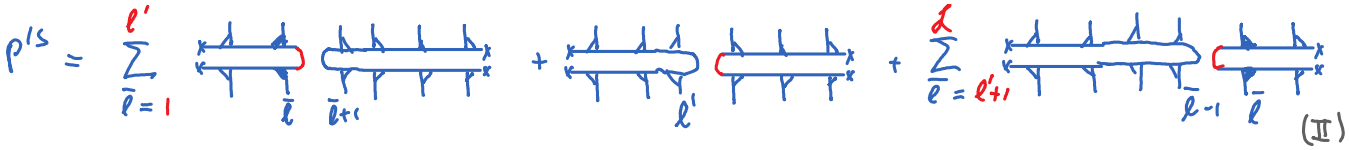

(II)

The three terms with $\bar{\ell} = \ell$, $\ell' = \ell$, $\bar{\ell} = \ell+1$, applied to $\hat{H}\,|\Psi(t)\rangle$, yield

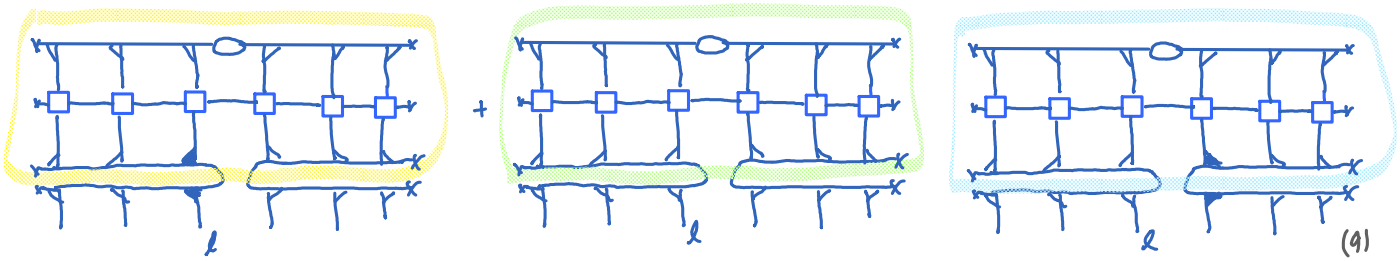

(9)

matching structure of (7). Thus, P^{ls}, applied to $H|\Psi(t)\rangle$, yields terms of precisely the right structure!

To integrate projected Schrödinger eq. (4), we write tangent space projector in the form (TS-I.5.26):

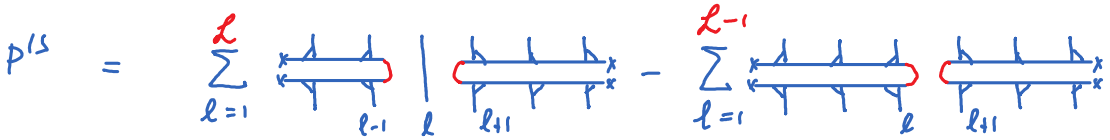

(10)

and write (4) as

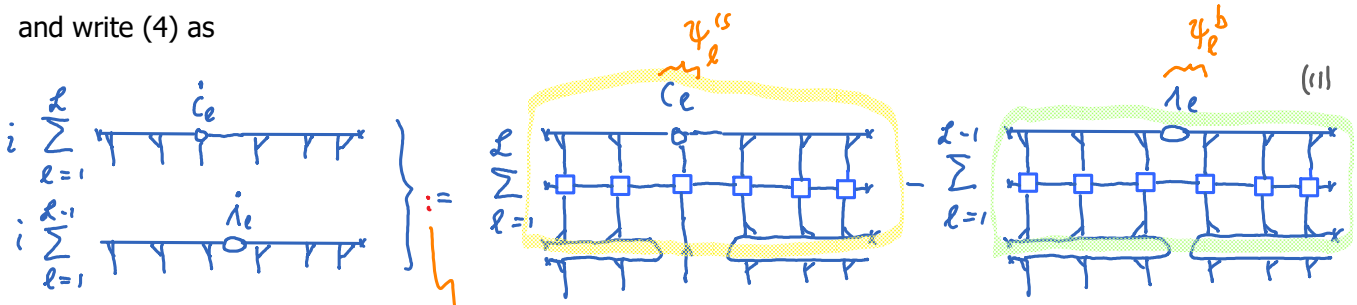

(11)

Right side is sum of terms, each specifying an update of one ψ^{ls}_ℓ or ψ^{b}_ℓ on the left. Eq. (4) can be integrated one site at a time, by defining the updates through the following local Schrödinger equations:

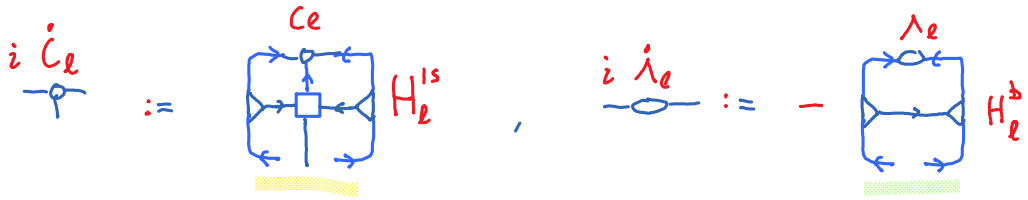

(12)

In site-canonical form, site ℓ involves two terms linear in C_ℓ : $\quad i\dot{C}_\ell(t) = H^{ls}_\ell C_\ell(t)$ (13)

Their contribution can be integrated exactly: replace $C_\ell(t)$ by $\quad C_\ell(t+\tau) = e^{-iH^{ls}_\ell \tau} C_\ell(t)$ (14)

forward time step

In bond-canonical form, site ℓ involves two terms linear in Λ_ℓ : $\quad i\dot{\Lambda}_\ell(t) = -H^{b}_\ell \Lambda_\ell(t)$ (15)

Their contribution can be integrated exactly: replace $\Lambda_\ell(t)$ by $\quad \Lambda_\ell(t-\tau) = e^{iH^{b}_\ell \tau} \Lambda_\ell(t)$ (16)

backward(!) time step

In practice, $e^{-i H_\ell^{IS} \tau} C_\ell$ and $e^{i H_\ell^{b} \tau} \Lambda_\ell$ are computed by using Krylov methods.

Build a Krylov space by applying H_ℓ^{IS} multiple times to C_ℓ, set up the tridiagonal representation $[H_\ell^{IS}]_{Krylov}$ of H_ℓ^{IS} in this basis, then compute the matrix exponential in this basis, and apply result to C_ℓ.
Likewise for H_ℓ^b and Λ_ℓ.

To successively update entire chains, alternate between site- and bond-canonical form, propagating forward or backward in time with H_ℓ^{IS} or H_ℓ^b, respectively:

1. Forward sweep, for $\ell = 1, \ldots, \mathcal{L}-1$, starting from $C_1(t) := \Gamma_1(t) B_2(t) \ldots B_\mathcal{L}(t)$ (17)

$C_\ell(t)\, B_{\ell+1}(t)$

$\xrightarrow[1(a)]{H_\ell^{IS}}$ $C_\ell(t+\tau)\, B_{\ell+1}(t)$ (1(b))

$= A_\ell(t+\tau)\, \tilde{\Lambda}_\ell(t+\tau)\, B_{\ell+1}(t)$

$\xrightarrow[1(c)]{H_\ell^{b}}$ $A_\ell(t+\tau)\, \tilde{\Lambda}_\ell(t)\, B_{\ell+1}(t)$ (1(d))

$= A_\ell(t+\tau)\, C_{\ell+1}(t)$

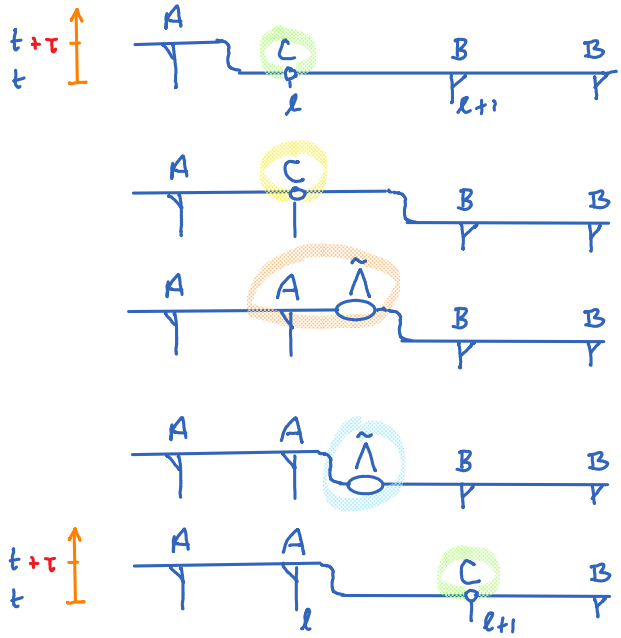

(18)

until we reach last site, and MPS described by $A_1(t+\tau) \ldots A_{\mathcal{L}-1}(t+\tau)\, C_\mathcal{L}(t)$ (19)

2. Turn around: $C_\mathcal{L}(t)$

$\xrightarrow[2(a)]{H_\mathcal{L}^{IS}}$ $C_\mathcal{L}(t+\tau)$

$\xrightarrow[2(b)]{H_\mathcal{L}^{IS}}$ $C_\mathcal{L}(t+2\tau)$

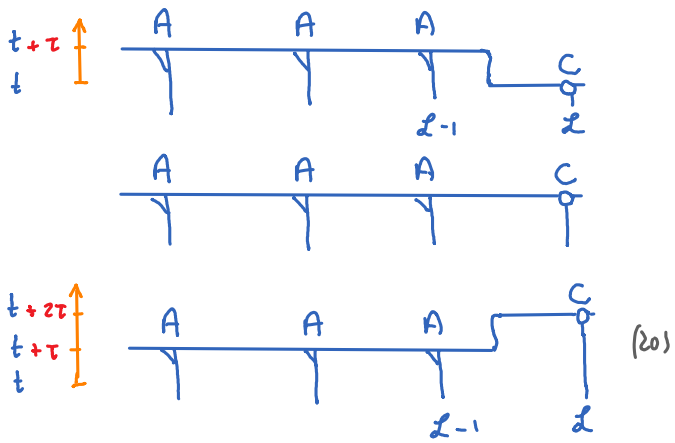

(20)

3. Backward sweep, for $\ell = \mathcal{L}-1, \ldots, 1$, starting from $A_1(t+\tau) \ldots A_{\ell-1}(t+\tau)\, C_\ell(t+2\tau)$ (21)

$A_\ell(t+\tau)\, C_{\ell+1}(t+2\tau)$

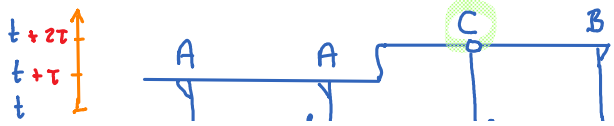

$$A_\ell(t+\tau)\,C_{\ell+1}(t+2\tau)$$

$$= \underset{3(a)}{} A_\ell(t+\tau)\,\tilde{\Lambda}_\ell(t+2\tau)\,B_{\ell+1}(t+2\tau)$$

$$\xrightarrow[3(b)]{H_\ell^b} A_\ell(t+\tau)\,\hat{\Lambda}_\ell(t+\tau)\,B_{\ell+1}(t+2\tau)$$

3(c)

$$= C_\ell(t+\tau)\,B_{\ell+1}(t+2\tau)$$

$$\xrightarrow[3(d)]{H_\ell^{IS}} C_\ell(t+2\tau)\,B_{\ell+1}(t+2\tau)$$

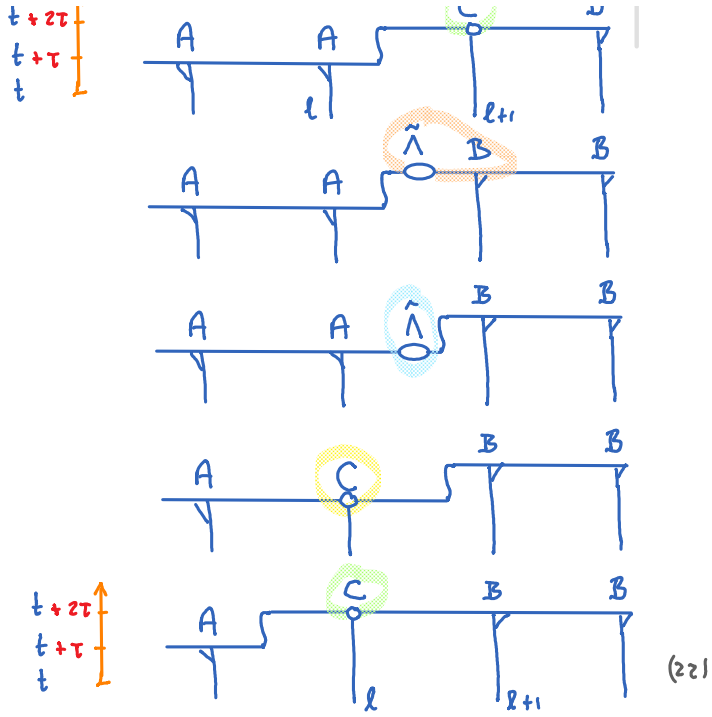

(22)

until we reach first site, and MPS described by $C_1(t+2\tau)\,B_2(t+2\tau)\ldots B_L(t+2\tau)$ (23)

The scheme described above involves 'one-site updates'. This has the (major!) drawback (as in one-site DMRG), that it is not possible to dynamically explore different symmetry sectors. To overcome this drawback, a 'two-site update' version of tangent space methods can be set up [Haegemann2016, App. C].

A systematic comparison of various MPS-based time evolution schemes has been performed in [Paeckel2019]. Conclusion: 2-site-update tangent space scheme is most accurate!

A scheme for doing 1-site TDVP while nevertheless expanding bonds, called 'controlled bond expansion (CBE), was proposed in [Li2022] (see next lecture!).

2. 2-site projectors P^{2s}

The construction of tangent space $\mathbb{V}^{1s}$ and its projector P^{1s} can be generalized to n sites [Gleis2022a].

We focus on $n = 2$ (but general case is analogous). Define space of 2-site variations:

$\mathbb{V}^{2s}$ = span of all states $|\Psi'\rangle$ differing from $|\Psi\rangle$ on precisely 2 neighboring sites

$$= \mathrm{span}\left\{ |\Psi'\rangle = \; \text{(2 sites at } \ell,\ell+2\text{)}, \ell \in [1, \mathcal{L}-1] \right\} \tag{1}$$

formal definition:

$$= \mathrm{span}\left\{ \mathrm{im}\left(P^{2s}_\ell\right) \;|\; \ell \in [1, \mathcal{L}-1] \right\} \tag{2}$$

(im: image)

Recall:

local 2s projector: $\ell \in [1, \mathcal{L}-1]$

$$\hat{P}^{2s}_\ell = \text{(TS-I.4.9)} \tag{3}$$

Global 2s projector $\hat{P}^{2s}$, such that $\mathbb{V}^{2s} = \mathrm{im}\left(P^{2s}\right)$, can be found with a Gram-Schmidt scheme analogous to our construction of $\hat{P}^{1s}$, see [Gleis2022a]:

compare (TS-I.5.22)

$$P^{2s} := \sum_{\ell=1}^{\ell'-1} \underbrace{P^{2s}_{\ell}}_{\ell<} - P^{1s}_{\ell+1} = P^{DK}_{\ell,\ell+2} + P^{2s}_{\ell'} + \sum_{\ell=\ell'+1}^{\mathcal{L}-1} \underbrace{P^{2s}_{\ell}}_{\ell>} - P^{1s}_{\ell} = P^{KD}_{\ell-1,\ell+1} \quad \text{for any } \ell' \in [1, \mathcal{L}-1] \tag{4}$$

$$P^{2s} = \sum_{\ell=1}^{\ell'-1} \; \text{(ℓ, ℓ+2)} + \; \text{(ℓ')} + \sum_{\ell=\ell'+1}^{\mathcal{L}} \; \text{(ℓ−1, ℓ+1)} \tag{5}$$

All summands are mutually orthogonal, ensuring that $(P^{2s})^2 = P^{2s}$, and that $P^{2s} P^{2s}_{\ell'} = P^{2s}_{\ell'}$. (6)

Alternative expression:
compare (TS-I.5.26)

$$P^{2s} = \sum_{\ell=1}^{\mathcal{L}-1} P^{2s}_\ell - \sum_{\ell=1}^{\mathcal{L}-2} P^{1s}_{\ell+1} = \sum_{\ell=1}^{\mathcal{L}-1} \; \text{(ℓ)} - \sum_{\ell=1}^{\mathcal{L}-2} \; \text{(ℓ+1)} \tag{7}$$

This projector is used for 2-site TDVP (see TS-II.3)

Orthogonal n-site projectors

For any given MPS $|\Psi[M]\rangle$, full Hilbert space of chain can be decomposed into mutually orthogonal subspaces:

$$\mathbb{V} = V_1 \otimes \dots \otimes V_\ell = \bigoplus_{n=0}^{\ell} \mathbb{V}^{n\perp} \tag{8}$$

with $\mathbb{V}^{0\perp} := \mathbb{V}^{0s} := \mathrm{span}\{|\Psi\rangle\}$ (9)

'irreducible' $\mathbb{V}^{n\perp}$ is complement of $\mathbb{V}^{(n-1)s}$ in $\mathbb{V}^{ns} = \mathbb{V}^{(n-1)s} \oplus \mathbb{V}^{n\perp}$ (10)

= span of states differing from $|\Psi\rangle$ on n contiguous sites, not expressible through subsets of $n' < n$ sites

Correspondingly, identity can be decomposed as:

$$\mathbb{1}_{\mathbb{V}} = \mathbb{1}_d^{\otimes \ell} = \sum_{n=0}^{\ell} P^{n\perp} \quad , \quad P^{n\perp} P^{n'\perp} = \delta^{nn'} P^{n\perp} \tag{11}$$

completeness; orthogonality

where $P^{\perp n}$ is defined as the projector having $\mathbb{V}^{n\perp}$ as image: $\mathrm{im}(P^{n\perp}) = \mathbb{V}^{n\perp}$ (12)

$$P^{0\perp} = P^{0s} := |\Psi\rangle\langle\Psi| =$$ 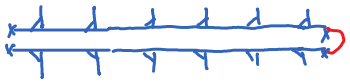 (13)

$$n \geq 1: \quad P^{n\perp} := P^{ns}\left(\mathbb{1}_{\mathbb{V}} - P^{(n-1)s}\right) = P^{ns} - P^{(n-1)s} \tag{14}$$

since $\mathbb{V}^{(n-1)s} \subset \mathbb{V}^{ns} \Rightarrow \mathrm{im}(P^{(n-1)s}) \subset \mathrm{im}(P^{ns})$
$\Rightarrow P^{ns} P^{(n-1)s} = P^{(n-1)s}$

Consider n=1:

$$P^{1\perp} = P^{1s} - P^{0s}$$

(TS-I.5.26)

$$= \sum_{\ell=1}^{\ell'}$$ 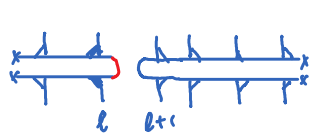 $$+$$ 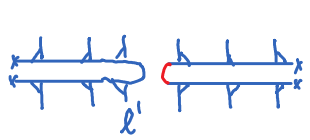 $$+ \sum_{\ell=\ell'+1}^{\ell}$$ 

choose $\ell' = \ell$ $-$  (15)

$$= \sum_{\ell=1}^{\ell}$$ 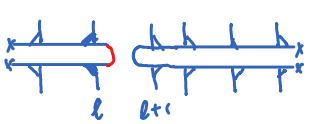 $$= \sum_{\ell=1}^{\ell} P^{\mathbb{D}k}_{\ell,\ell+1}$$

projects onto all 1-site variations orthogonal to $|\Psi\rangle$ (16)

Consider n=2:

(TS-I.4.17) $P^{0s}_{\ell+1}$

$$P^{2\perp} = P^{2s} - P^{1s} = \left(\sum_{\ell=1}^{\ell-1} P^{2s}_{\ell} - \sum_{\ell=2}^{\ell-1} P^{1s}_{\ell}\right) - \left(\sum_{\ell=1}^{\ell} P^{1s}_{\ell} - \sum_{\ell=1}^{\ell-1} P^{b\,\prime\prime}_{\ell}\right) \tag{17}$$

move P^{1s}_{ℓ} from 3rd to 2nd term

$$= \sum_{\ell=1}^{\ell-1}\left(P^{2s}_{\ell} - P^{1s}_{\ell+1} - P^{1s}_{\ell} + P^{0s}_{\ell+1}\right) \tag{18}$$

$$= \sum_{\ell=1}^{\ell-1}\Big($$ 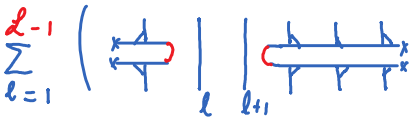

(19)

(TS-I.3.28)

$$= \sum_{\ell=1}^{L-1} \quad \ell \quad \ell+1 \quad = \sum_{\ell=1}^{L-1} P^{DD}_{\ell,\ell+1}$$

very important result! (20)

3. 2-site TDVP (optional)

TS-II.3

[Haegeman2016, Sec. V & App. C]

2-site tangent space methods are analogous to 1-site methods, but use a 2-site projector. There is a conceptual difference, though: the main reason for using 2-site schemes is that they allow sectors with new quantum numbers to be introduced if the action of H requires this. However, states with different ranges of quantum numbers live in different manifolds, hence this procedure 'cannot easily be captured in a smooth evolution described using a differential equation. However, like most numerical integration schemes, the aforementioned algorithm is intrinsically discrete by choosing a time step, and it poses no problem to formulate an analogous two-site algorithm'. [Haegeman2016, Sec. V]. In other words: the tangent space approach is conceptually not as clean for the 2-site as for the 1-site scheme.

Schrödinger equation, projected onto 2-site tangent space, now takes the form

$$i \frac{d}{dt} |\psi[M(t)]\rangle = \hat{P}^{2s} \hat{H} |\psi[M(t)]\rangle$$

$\hat{P}^{2s}$ =

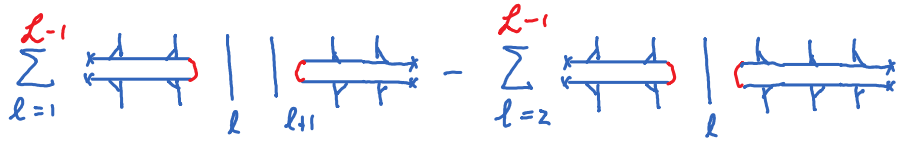

This yields [compare (1.11)]:

or

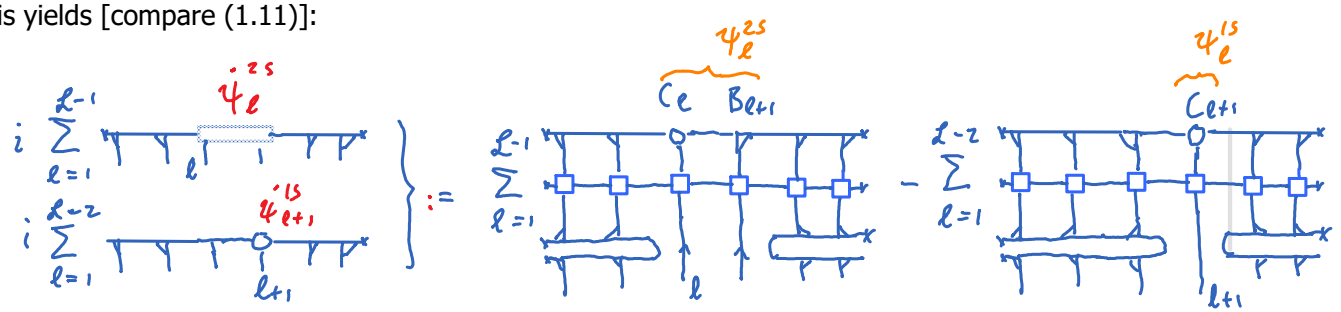

Right side is sum of terms, each specifying an update of one ψ_ℓ^{2s} or ψ_ℓ^{1s} on the left. Eq. (4) can be integrated one site at a time, by defining the updates through the following local Schrödinger equations:

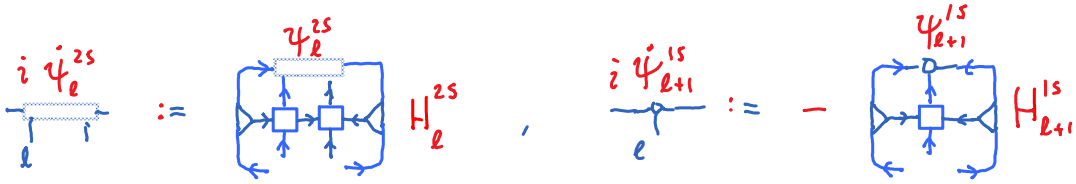

Right side is sum of terms, each linear in a factor appearing on the left. Can be integrated one site at a time:

In 2-site-canonical form, site ℓ involves two terms linear in ψ_ℓ^{2s} : $i \dot{\psi}_\ell^{2s}(t) = H_\ell^{2s} \psi_\ell^{2s}(t)$ (10)

Their contribution can be integrated exactly: replace $\psi_\ell^{2s}(t)$ by $\psi_\ell^{2s}(t+\tau) = e^{-i H_\ell^{2s} \tau} \psi_\ell^{2s}(t)$ (11)

forward time step

In 1-site-canonical form, site $\ell+1$ involves two terms linear in $\psi_{\ell+1}^{1s}$: $i \dot{\psi}_{\ell+1}^{1s}(t) = -H_{\ell+1}^{1s} \psi_{\ell+1}^{1s}(t)$ (12)

Their contribution can be integrated exactly: replace $\psi_{\ell+1}^{1s}(t)$ by $\psi_{\ell+1}^{1s}(t-\tau) = e^{i H_{\ell+1}^{1s} \tau} \psi_{\ell+1}^{1s}(t)$ (13)

Their contribution can be integrated exactly: replace $\psi^{1s}_{\ell+1}(t)$ by $\psi^{1s}_{\ell+1}(t-\tau) = e^{iH^{1s}_{\ell+1}\tau}\,\psi^{1s}_{\ell+1}(t)$ (13)

backward(!) time step

To successively update entire chains, alternate between 2-site- and 1-site-canonical form, propagating forward or backward in time with H^{2s}_{ℓ} or H^{1s}_{ℓ}, respectively (analogously to 1-site scheme).

A systematic comparison of various MPS-based time evolution schemes has been performed in [Paeckel2019]. Conclusion: 2-site-update tangent space scheme is most accurate!

4. Energy variance [Hubig2018]

TS-II.4

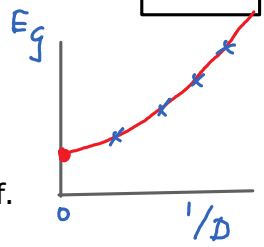

When doing MPS computations involving SVD truncations of virtual bonds, the results should be computed for several values of the bond dimension, D, to check convergence as $D \to \infty$. Often it is also necessary to extrapolate the results to $D = \infty$, e.g. by plotting results versus $1/D$ or some power thereof.

However, for some computational schemes, it is not *a priori* clear how the observable of interest scales with D, nor how it should be extrapolated to $D = \infty$. An example is ground state energy when computed using 1-site DMRG with subspace expansion [Hubig2015], because it does not rely on SVD truncation of bonds.

Thus, it is of interest to have a reliable error measure without requiring costly 2-site DMRG. A convenient scheme was proposed in [Hubig2018], based on a smart way to approximate the full energy variance,

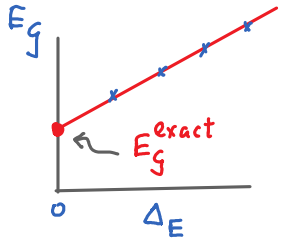

$$\Delta_E := \|(H - E)|\psi\rangle\|^2 = \langle\psi|(\hat{H} - E)^2|\psi\rangle \quad (= \text{zero for an exact eigenstate}) \quad (1)$$

$$= \langle\psi|\hat{H}^2|\psi\rangle - E^2, \quad \text{with} \quad E = \langle\psi|\hat{H}|\psi\rangle \quad (2)$$

Then extrapolations can be done by computing quantity of interested for several D, but plotting the results via Δ_E, and extrapolating to $\Delta_E \to 0$

If quantity of interest is energy, then extrapolation is linear, $E_g(\Delta_E) = E_g^{exact} + a \cdot \Delta_E$ (3)

Computing $\langle\psi|\hat{H}^2|\psi\rangle$ directly is costly for large systems with long-ranged interactions, such as 2D systems treated by DMRG snakes. Also, computing Δ_E as the difference between two potentially large numbers is prone to inaccuracies. [Hubig2018] found a computation scheme in which the subtraction of such large numbers is avoided *a priori*.

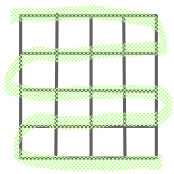

Key idea: use projectors $P^{n\perp}$ onto mutually orthogonal, irreducible spaces $V^{n\perp}$

Recall (2.11): $\mathbb{1}_V = \mathbb{1}_d^{\otimes \mathcal{L}} = \sum_{n=0}^{\mathcal{L}} P^{n\perp}$, $P^{n\perp} P^{n'\perp} = \delta^{nn'} P^{n\perp}$ (5)

completeness (4) orthogonality

with $P^{0\perp} = |\Psi\rangle\langle\Psi|$ (6)

(2.16) $P^{1\perp} = \sum_{l=1}^{\mathcal{L}}$ 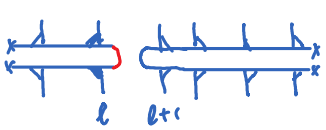

,

(2.17) $P^{2\perp} = \sum_{l=1}^{\mathcal{L}}$ 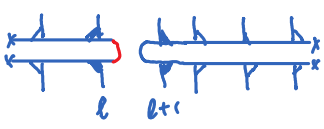

(7)

Insert completeness into definition of variance: $\Delta_E \overset{(4)}{=} \langle\psi|(\hat{H} - E)\sum_{n=0}^{\mathcal{L}} P^{n\perp}(\hat{H} - E))|\psi\rangle =: \sum_{n=0}^{\mathcal{L}} \Delta_E^{n\perp}$ (8)

Now two crucial simplifications occur:

$\Delta_E^{0\perp} \overset{(5)}{=} \langle\psi|(\hat{H} - E)|\psi\rangle\langle\psi|(\hat{H} - E))|\psi\rangle = (E - E)(E - E) = 0$ (9)

largest contribution to variance cancels by construction!

$$\Delta_E^{0\perp} \overset{(5)}{=} \langle\psi|(\hat{H}-E)\underbrace{|\psi\rangle\langle\psi|}_{(6)\ P^{0\perp}}(\hat{H}-E)|\psi\rangle = (E-E)(E-E) = 0 \tag{9}$$

largest contribution to variance cancels by construction!

$n>0$

$$\Delta_E^{n\perp} = \langle\psi|(\hat{H}-E)P^{n\perp}(\hat{H}-E)|\psi\rangle = \langle\psi|\hat{H}\underbrace{P^{n\perp}P^{n\perp}}_{=P^{n\perp}}\hat{H}|\psi\rangle, \quad \text{since } P^{(n>0)\perp}|\psi\rangle \overset{(5,6)}{=} 0 \tag{10}$$

(TS-II.2.11)

$$= \| P^{n\perp}\hat{H}|\psi\|^2 \tag{11}$$

In practice, approximate Δ_E by the first two nonzero terms:

$$\Delta_E \simeq \Delta_E^{2s} = \Delta_E^{1\perp} + \Delta_E^{2\perp} = \boxed{\langle\psi|\hat{H}P^{1s}\hat{H}|\psi\rangle + \langle\psi|\hat{H}P^{2s}\hat{H}|\psi\rangle} \tag{12}$$

(11) is exact if longest-range terms in $\hat{H}$ are nearest-neighbor, because then $P^{(n\geq 3)\perp}\hat{H}|\Psi\rangle = 0$ (13)

Explicit computations:

$n=1$: Recall $P^{1\perp} \overset{\text{(TS-II.2.16)}}{=} \sum_{\ell=1}^{\mathcal{L}}$ 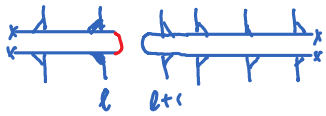 $= \sum_{\ell=1}^{\mathcal{L}} P^{DK}_{\ell,\ell+1}$ (14)

mutually orthogonal! (TS-I.4.15)

$$\Delta_E^{1\perp} = \langle\psi|\hat{H}\underbrace{P^{1\perp}P^{1\perp}}_{\sim}\hat{H}|\psi\rangle = \|P^{1\perp}H\psi\|^2 = \sum_{\ell=1}^{\mathcal{L}}\|P^{DK}_{\ell,\ell+1}H\psi\|^2 \tag{15}$$

$= \sum_{\ell=1}^{\mathcal{L}}$ 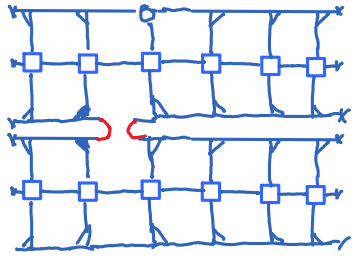 $= \sum_{\ell=1}^{\mathcal{L}}$ 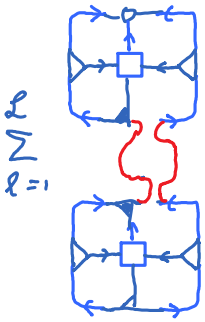 $= \sum_{\ell=1}^{\mathcal{L}}$ 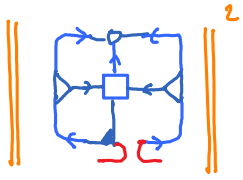 (16)

We would like to avoid computing  explicitly, because of its large image dimension.

So rewrite, using isometry condition for discarded sector:  (17)

and completeness of kept together with discarded isometries:  (18)

$= \sum_{\ell=1}^{\mathcal{L}}$ 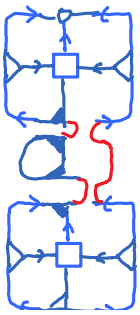 $= \sum_{\ell=1}^{\mathcal{L}}$ 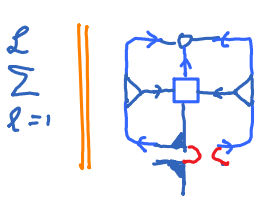 $= \sum_{\ell=1}^{\mathcal{L}}$ 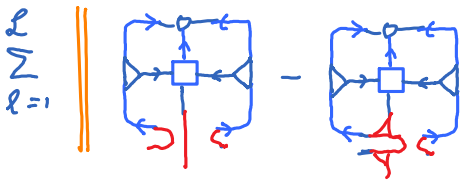

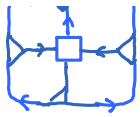

(19)

$n = 2$: Recall $P^{2\perp} \overset{(2.17)}{=} \sum_{\ell=1}^{\mathcal{L}-1}$ 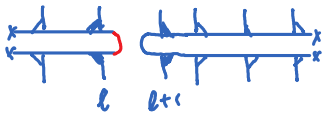 $= \sum_{\ell=1}^{\mathcal{L}} P^{DD}_{\ell,\ell+1}$ (20)

$\Delta_E^{2\perp} = \langle \psi | \hat{H} \underbrace{P^{2\perp} P^{2\perp}} \hat{H} | \psi \rangle = \| P^{2\perp} H \psi \|^2 = \sum_{\ell=1}^{\mathcal{L}-1} \| P^{D}_{\ell,\ell+1} H \psi \|^2$ (21)

$= \sum_{\ell=1}^{\mathcal{L}-1}$ 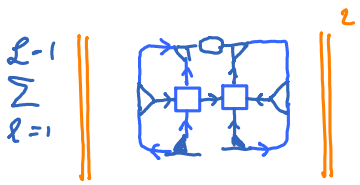 $=$ 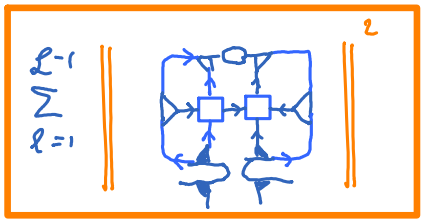 (22)

again use  (23)